

RESEARCH ARTICLE

Intelligent Health Diagnosis of Lithium Battery Pole Double Rolling Equipment Driven by Hybrid BP Neural Network and Expert System

YANJUN XIAO^{1,2,3}, SHUHAN DENG^{1,3}, FURONG HAN^{2,3}, XIAOLIANG WANG^{1,3},
YUNFENG JIANG^{1,3}, AND KAI PENG³

¹Tianjin Key Laboratory of Power Transmission and Safety Technology for New Energy Vehicles, School of Mechanical Engineering, Hebei University of Technology, Tianjin 300401, China

²Career Leader Intelligent Control Automation Company, Suqian, Jiangsu 223800, China

³School of Mechanical Engineering, Hebei University of Technology, Tianjin 300401, China

Corresponding authors: Yanjun Xiao (xyj@hebut.edu.cn), Yunfeng Jiang (hebutwf123@163.com), and Kai Peng (h313930@163.com)

This work was supported in part by the Jiangsu Province Training Fund under Grant BRA2020244 and the Natural Science Foundation of Hebei Province under Grant E2022202136.

ABSTRACT At present, the fault diagnosis methods of lithium battery pole rolling mill mostly rely on manual experience and the self-test function of mature control devices such as frequency converters and lack the ability of intelligent fault diagnosis for the whole equipment and the ability to evaluate the health state of the equipment during operation. To improve the intellectual health diagnosis ability of lithium battery pole double rolling mill equipment, starting from the structure and technology of lithium battery pole double rolling equipment, this paper analyzes its common fault types. It summarizes the shortcomings and common fault types of existing equipment. Then, we introduce fuzzy reasoning into the fault diagnosis method based on Expert Systems and establish the FEFDM of lithium battery pole double rolling equipment. Finally, we introduce the concept of health degree, effectively connect BP neural network and health degree through the fuzzy set, and establish an equipment operation health state evaluation method based on an improved BP Neural Network, which realizes the evaluation ability of the health state of double roller equipment. In addition, we use Extended Kalman Filtering (EKF) to clean the “dirty data” and filter out the Gaussian white noise from the signal. The health diagnosis method proposed in this paper can meet the ability to accurately locate and diagnose the fault of lithium battery pole double roller equipment and evaluate the health state of equipment operation and maintain the equipment in advance.

INDEX TERMS Compound fault diagnosis, health status assessment, BP neural network, FEFDM.

I. INTRODUCTION

With the rapid growth of new energy vehicle sales, the global lithium battery production continues to maintain a fast growth form, and the speed of relevant technological innovation in the industry continues to improve [1]. The global lithium battery market scale and demand trend are shown in Fig.1. According to the data, the lithium battery industry proliferates every year. By the end of 2016, the global sales of new energy vehicles had exceeded 510 thousand, and the lithium battery market was about 81.3 billion yuan. The demand for

power batteries was about 47.6 billion yuan, a year-on-year increase of 58.7%. According to the statistics in Fig.1, the global lithium battery capacity reached 104 GWh in 2016. In 2020, the demand for lithium batteries will get five times that of 2015. It is estimated that the scale of the global lithium battery industry will reach about 48.7 billion dollars by 2022. Therefore, as the core component of electric vehicles, lithium battery still has significant demand. It is essential to optimize lithium batteries' production and assembly [2].

As the lithium battery pole piece double rolling equipment responsible for the production of lithium battery pole piece belt in the production process of lithium battery, it is also facing new opportunities and challenges. The traditional

The associate editor coordinating the review of this manuscript and approving it for publication was Baoping Cai¹.

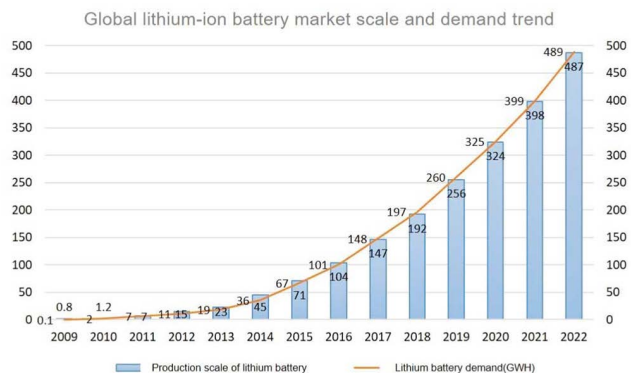


FIGURE 1. Global Lithium-ion Battery market size and demand trend.

lithium battery pole double rolling equipment has a high level of automation, which can realize the automatic rolling production process of the lithium battery pole strip [3]. The control system of double roller equipment is more complex than that of single roller equipment, and there is a strong coupling relationship between multiple control elements. Therefore, in the continuous rolling process of battery pole double rolling equipment, with the increase of rolling working time and the change of internal conditions and external environment of the equipment, failure and “Sub-Health” state which is not conducive to the regular operation of the equipment will inevitably occur [4], [5]. Combined with the background of current industry 4.0 and conforming to the development trend of the intelligent manufacturing industry, it is urgent to improve the intellectual level of lithium battery pole double roller equipment, reduce equipment faults and sub-health status, and apply health diagnosis technology to lithium battery pole double roller equipment [6].

Lithium battery pole piece rolling mill equipment first appeared in the 1970s, controlled by an advanced hydraulic servo system. Ji *et al.* [7] adopted AGC hydraulic servo control system produces pole rolling force between 100-300T cruising speed between 90-120 M / min. The rolling mill equipment has high control accuracy and self-monitoring function to realize the equipment’s fault diagnosis and state detection function. Although the control effect is perfect, its diagnosis is mainly aimed at the hydraulic part of the equipment. The diagnosis effect of the overall state of the equipment, sensors, and other factors is not high, and the system cost is expensive. After that, the lithium battery pole chip control system with PLC as the core appeared suitable for application in complex industrial sites. To solve the curacy decline caused by friction heating, Zhao *et al.* [8] developed a new type of unwinding roll movement structure based on the traditional lithium electric mill, and realized multi-axis control by PLC controller. However, most of the fault diagnosis functions of this equipment are realized through the self-detection part of PLC and mature rules such as frequency converter. They lack the overall fault diagnosis of the equipment and do not have the health status [9].

Fault diagnosis technology is a comprehensive cross-technology formed and developed to meet equipment production needs [10]. It has experienced from the diagnosis stage based on manual field experience to the diagnosis stage based on sensor signal detection technology [11], [12]. With the development of information acquisition and processing technology, the new intelligent diagnosis technology constructs the brilliant fault diagnosis model and method based on the traditional sensor signal acquisition method and the smart machine learning algorithm. The fault diagnosis system is often composed of a monitoring system with the computer as the information processing and monitoring center and a diagnosis strategy with an Expert System, Neural Network, Support Vector Machine, and other fusion or improved algorithms as the center [13]. He and He [14] proposed the use of short-time Fourier transform (STFT) to pre-process sensor signals, and constructed an optimized deep learning structure, the mass memory storage retrieval (LAMSTAR) neural network, for bearing fault diagnosis based on the simple spectral matrix obtained from STFT. The mechanical design of rolling mill equipment is complex, and the fault point is difficult to locate accurately. As the crucial part of the rolling mill, roll determines the whole process from extrusion to forming [15]. Aiming at the particularity of rolling mill bearing vibration signal, Zhao *et al.* [16] proposed a fault diagnosis method combining AMVMD (Adaptive Multivariable Variational Modal Decomposition) and MCLDCNN (Multi-Channel One-Dimensional Convolutional Neural Network), which solves the problems of insufficient data and low diagnostic accuracy in the fault diagnosis of multi-row bearings such as rolling mills. The failure of the rolling mill may also be caused by other factors, such as the axis of the roll [17], the drive shaft [18], the gear [19], and the hydraulic system [20].

With the vigorous development of fault diagnosis technology, the traditional fault diagnosis theory with fault as the primary research object began to transfer to the state analysis of equipment operation [21]. The United States first tried to predict the operation degree of equipment in the aerospace field and invented an intelligent maintenance system with deterioration monitoring technology, fault prediction technology, and intelligent maintenance technology as the core [22]. After that, the PHM technology (Fault Prediction and Health Management) appeared. This technology introduces the concept of fault prediction based on the diagnosis of the original fault. It predicts the possible defects of the equipment and the operation state of the equipment in advance, which is used to judge the service life of the equipment [23]. Many scholars have put forward novel methods to evaluate the operation status of rolling equipment, such as hot continuous rolling mills and finishing mills. Li [24] had made detailed research on some machine learning algorithms, hybrid hidden Markov model, neural network, knowledge reasoning methods, and other theories, which provides a good idea for the follow-up research of health management technology. Fu *et al.* [25] calculated the envelope of the original rolling

pressure data through the sliding window mean filtering method to diagnose and give feedback on the problems of rolling pressure measurement accuracy, the size difference of the main roll contact pad, and maintenance of primary bearing support, which is of great significance to maintaining the accuracy and equipment pre-maintenance of the hot continuous rolling mill. Qiao *et al.* [26] proposed a multi-objective optimization method based on adaptive coupled neurons to enhance mechanical early failure features to overcome the disadvantage of using useless noise techniques to suppress blindly and eliminate noise and easily remove weak useful features closely related to mechanical health status. The commonly associated technologies are primarily concentrated in steel rolling and other similar fields, and the health diagnosis of key components of multiple rolling mills has been realized [27]. Sun [28] started with the health status of the rolling mill in the working process, establishes a diagnosis method of the rolling mill working health status by using fuzzy theory and deep confidence network method, realizes the health status evaluation function of the rolling mill working process, determines the health status level of the rolling mill running process and gives the operation and maintenance decision by comparing the health status degree table.

To sum up, the current research on health diagnosis of lithium battery pole strip mill has the following problems:

(1) Some deep learning, migration learning, and reinforcement learning methods require large amounts of labeled data, long model training time, and weak generalization and portability of the models. Complex models require more considerable development costs, and fault diagnosis models cannot correlate well with field monitoring equipment.

(2) However, there are many technical differences related to the steel strip, such as the accuracy [29]. At present, the lithium battery pole double rolling equipment still lacks fault diagnosis technology for the whole kit and evaluation technology for the operation of the equipment.

(3) The fault diagnosis function of lithium battery pole piece rolling mill equipment is single, which only diagnoses whether individual electrical parts can work normally, and lacks in-depth research on the overall operation state of the equipment in the production process.

(4) The lithium battery pole piece double rolling equipment lacks a health status evaluation method for equipment operation. In most cases, the evaluation of equipment status depends on the subjective experience judgment of professional technicians, and there is a lack of health status evaluation method of lithium battery pole piece double rolling equipment based on quantitative prediction method.

We deeply study the lithium battery pole double rolling equipment given the above problems. Aiming at the problems of its control system and mechanical mechanism, complex fault types, and low equipment reuse rate, we design a fault diagnosis method for lithium battery pole double rolling equipment based on FEFDM and a health state evaluation method for lithium battery pole double rolling equipment based on improved neural network, The combination of the

two forms the health diagnosis method proposed in this paper. The diagnosis method realizes the rapid diagnosis of the fault location of the equipment and the healthy state of the equipment to ensure the stability of the long-term control performance of the lithium battery electrode.

Firstly, we analyze the failure of lithium battery pole double rolling equipment. The common fault types of the lithium battery pole double rolling equipment are summarized by a detailed analysis of the equipment structure, rolling process, and control elements of the lithium battery pole double rolling equipment. The overall framework of the health diagnosis method is established.

Secondly, aiming at the fault types of battery pole double rolling equipment, we propose a fault diagnosis method of lithium battery pole double rolling equipment based on the fuzzy expert system. This method combines fuzzy theory with expert system theory, establishes a fuzzy expert knowledge database and fuzzy reasoning mechanism, and realizes the fuzzy reasoning of the general fault of double roller equipment.

Finally, aiming at the problem that the lithium battery pole double rolling fault diagnosis system cannot distinguish the health state of equipment, the concept of health degree is introduced on the original basis, and a health state evaluation method of lithium battery pole double rolling equipment based on Fuzzy BP Neural Network is proposed. This method effectively connects fuzzy logic with the BP Neural Network and health degree through unclear membership function to distinguish sub-health and fault states of double roller equipment.

The intelligent health diagnosis method of battery pole double rolling equipment driven by Hybrid BP Neural Network Expert System has the following innovations:

1. To evaluate the overall operation state of lithium battery pole double rolling equipment, this paper summarizes the composite fault type of lithium battery pole double rolling equipment by analyzing its equipment structure, rolling process, equipment control components and considering the strong coupling relationship between mechanical parts.

2. To solve the problem that the overall fault diagnosis accuracy of lithium battery pole double rolling equipment is not high, this paper introduces fuzzy reasoning into the fault diagnosis method based on the expert system, and establishes the FEFDM of lithium battery pole double rolling equipment. The fault diagnosis method makes the equipment have the ability to accurate fault diagnosis and lays a foundation for establishing subsequent health status evaluation methods.

3. To solve the problem that the lithium battery pole double rolling equipment cannot evaluate the health status of the equipment at present, the concept of health degree is introduced in this paper, and the BP neural network and health degree are effectively connected through the fuzzy set. This paper distinguishes the health, sub-health, and fault, states of the equipment, establish the equipment operation health state evaluation method based on an improved neural network, and realizes the evaluation ability of the health state of double

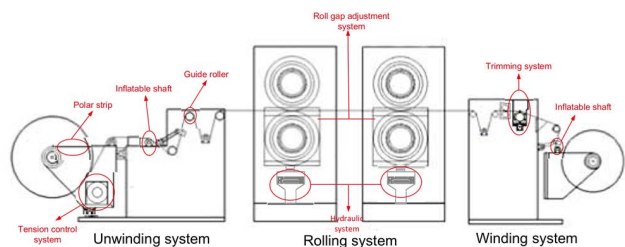


FIGURE 2. Structure diagram of lithium battery pole piece double rolling equipment.

roller equipment. In this paper, the health status evaluation method of double rolling equipment is combined with the fault diagnosis method to form the health diagnosis method of lithium battery pole double rolling mill equipment.

The paper is organized as follows: in section II, we analyzed the failure mechanism of lithium battery pole double rolling equipment, including the rolling system, unwinding system, and winding system. In section III, we have established a fault classification and location method based on FEFDM and a fuzzy knowledge base, database, and inference engine. In section IV, we propose a BP neural network health evaluation method and establish a three-phase fuzzy health mapping model to realize rolling mill equipment’s health diagnosis and evaluation. In section V, we carried out experimental verification.

II. FAILURE MECHANISM ANALYSIS

A. PROCESS FLOW ANALYSIS

The lithium battery pole piece double rolling equipment is mainly composed of three parts: unwinding system, rolling system, and winding system, as shown in Fig.2 [30]. The rolling system will carry out secondary rolling of the lithium battery pole strip. Compared with the single rolling mill, the deformation of the pole strip is divided into two rolling to meet the requirements. This process reduces the rebound caused by the pole strip’s tension, reduces the pole strip’s internal stress, and can effectively improve the production speed and quality [31], [32]. Table 1 predefines the meaning of the symbols used in this paper.

The roll gap adjustment part is introduced into the rolling system to control the rolling accuracy of the roll, and the rolling pressure system is used to adjust the rolling pressure. The rolling speed of the two main rolling devices is different because the accuracy of the pole plate after two rolls is higher than that of one rolling. At this time, the pole strip between rolls will produce tension. The tension control system needs to be introduced to stabilize the pressure, and achieve the purposes of accurate position, slight tension fluctuation, and stable rolling force in the production process of battery pole strip, to the quality and production rate of pole strip. The unwinding and winding systems are the same as the single roller press equipment. Some scholars have analyzed their workflow in detail [33], [34], which is not described here.

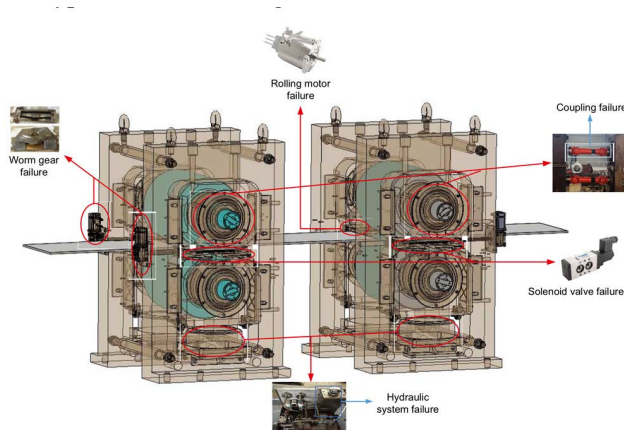


FIGURE 3. Schematic diagram of fault types of the rolling system.

B. FAULT ANALYSIS OF MAIN ROLLING SYSTEM

The rolling system is divided into rolling speed system fault, move gap adjustment system fault, and rolling pressure system fault according to the structure and process of lithium battery pole double rolling equipment. The specific fault types are shown in Fig.3 below.

1) ROLLING SPEED SYSTEM FAILURE

The fault types of rolling speed systems mainly include coupling fault and main roll motor fault. The coupling is a mechanical structure used to transmit torque and motor speed. The lithium battery pole double rolling equipment is responsible for transmitting the speed and torque of the main roll motor to the roll [35], as shown in Fig.3. As the pole piece rolling equipment is a rotating machine, the coupling will inevitably produce vibration under strong torque, which is easy to cause the coupling to loosen.

The control motor of the main roll is generally a three-phase asynchronous motor [36]. Long-term candle invasion of motor winding in the humid working environment or mechanical wear of coil will cause armature fault, and short circuit and the open circuit between motor boxes will cause the winding fault.

2) ROLL GAP ADJUSTMENT SYSTEM FAILURE

The fault types of roll gap adjustment system mainly include servo motor fault controlling its action and worm gear structure adjustment device fault [37]. Servo motor faults include the circuit burn out of the servo driver used to control the servo motor due to current impact, improper setting of driver reduction ratio, servo motor encoder fault, etc. The installation position of the worm structure adjustment device is shown in Fig.3. It is located at the inlet of the pole strip, so there are often faults such as gear wear and cracks.

3) ROLLING PRESSURE SYSTEM FAILURE

The faults of the rolling pressure system mainly include the responsibilities of the gas-liquid booster pump and solenoid

TABLE 1. Symbol definition.

Abbreviation	Term
FEFDM	Fuzzy Expert Fault Diagnosis Method
U	Fault symptom set
V	Fault cause set
$u_i (i = 1, 2, \dots, m)$	Fault symptom
$v_i (i = 1, 2, \dots, n)$	Fault cause
$A = \{a_1, a_2, \dots, a_n\}$	Fault cause weight set
$a_i (i = 1, 2, \dots, n)$	Weight coefficient
R_i	Diagnosis set of single fault causes
r_{ij}	The i -th element u_i in the fault symptom set corresponding to the j -th element v_j in the fault cause set
R	Fault cause diagnosis matrix
B	Fuzzy comprehensive diagnosis set
$b_j (j = 1, 2, \dots, n)$	Fuzzy operator
T	Pole piece tension
T'	Pole piece tension fluctuation
N	Magnetic particle brake torque
F	Rolling force
F'	Rolling force fluctuation
Q	Thickness of pole piece
v	Rolling speed
v'	Rolling speed fluctuation
P	Operating power of the trolling motor
S	The standard deviation of the tension value
m	The average value of tension value
n	The number of tension values
T_n	The n -th tension value
y_{ij}	Candidate reasoning result
λ	Threshold principle
HD	Health degree of lithium battery pole piece double rolling equipment
$x_i (i = 1, 2, \dots, n)$	Failure symptom parameters of rolling equipment
$f'(\cdot)$	Health degree mapping function
$\frac{A}{\%}$	Fuzzy subset
X	Health degree set
$I_i (i = 1, 2, \dots, 6)$	Number of input layer nodes
$O_i (i = 1, 2, 3)$	Number of output layer nodes
s	Number of hidden layer nodes
s^*	The optimal number of hidden layer nodes
$Accuracy_i$	Sample accuracy
$\overline{Accuracy}$	Average accuracy
TS	Tension sensor
FS	Pressure sensor
TOS	Torque sensor
THS	Thickness sensor
x_k	State equation

TABLE 1. (Continued.) Symbol definition.

z_k	Observation equation
$f(\cdot)$	Non-linear state function
$h(\cdot)$	Observation function
ω_k, c_k	Zero mean
Q_k, R_k	Uncorrelated white Gaussian noise
x_{k+1}	State equation at time $k + 1$
$\hat{x}_{k k}$	State estimate at time k
$P_{k k}$	Estimated covariance at time k
$\hat{x}_{k+1 k}$	One-step state estimate of state equation
$P_{k+1 k}$	One-step state estimation covariance
z_{k+1}	Observation equation at time $k + 1$
\hat{z}_{k+1}	One-step state estimate of observation equation
$P_{zz,k+1 k}$	Observation equation error covariance
$P_{xz,k+1 k}$	Cross-covariance matrix
K_{k+1}	State gain matrix
$\hat{x}_{k+1 k+1}$	State estimate at time $k + 1$
$P_{k+1 k+1}$	State estimation error covariance matrix at time $k + 1$
Y	Membership set

valve. Their installation positions are shown in Fig.3. The gas-liquid booster pump may fail to pressurize the two hydraulic cylinders due to the leakage of the sealing part of its one-way valve. The pole rolling equipment cannot provide sufficient rolling force and affect the accuracy of the pole strap. The solenoid valve in the rolling pressure system is used to control the gas-liquid booster pump. The magnetic pull of the solenoid valve coil may weaken or even fail, and the valve of the gas-liquid booster pump cannot be connected, resulting in equipment failure.

C. FAILURE ANALYSIS OF WINDING AND UNWINDING SYSTEM

In the winding and unwinding system, the battery pole strip may deviate and fold due to the interference factors of the equipment’s control system or the external environment. These factors will affect the quality and production rate of the pole strap. The specific fault types are shown in Fig.4.

1) FAILURE OF WINDING AND UNWINDING TENSION SYSTEM

The main faults of the winding tension system are the high temperature of the magnetic powder brake and the jamming of the magnetic powder brake. As the battery pole rolling equipment will generate a lot of heat when running at high speed, the friction will increase when the heat dissipation is insufficient [38]. This will lead to internal magnetic particle failure, magnetic particle brake failure, low output torque, and tension adjustment accuracy.

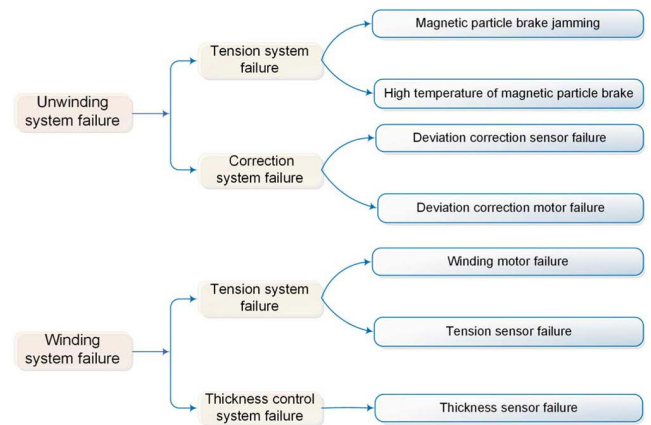


FIGURE 4. Schematic diagram of fault types of winding and unwinding system.

2) FAILURE OF WINDING AND UNWINDING DEVIATION CORRECTION SYSTEM

The faults of the winding and unwinding deviation correction system mainly include deviation correction sensor fault and deviation correction control motor fault. The deviation correction sensor may be due to the vibration generated by the rolling equipment during continuous operation, resulting in loose position deviation of the deviation correction sensor, resulting in inaccurate measurement results and other faults [39]. There may also be circuit faults inside the deviation correction sensor, which will lead to sensor damage in severe cases.

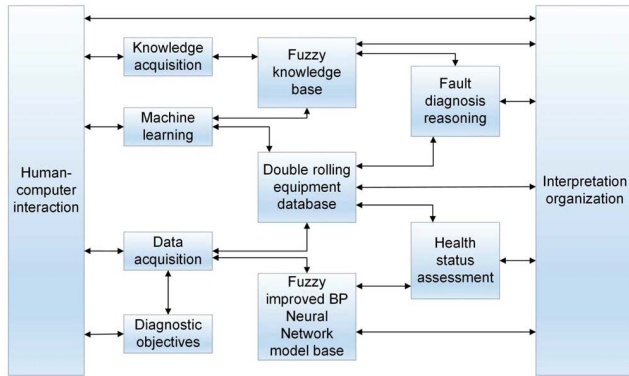


FIGURE 5. Lithium battery double pole frame diagnosis method.

3) FAILURE OF THICKNESS CONTROL SYSTEM

The fault of the thickness sensor mainly causes the responsibility of the thickness control system. Because the thickness control system precisely measures the real-time thickness through the laser thickness sensor and compares it with the set thickness. It controls the roll gap adjustment system and rolling pressure system in the main rolling system through the control algorithm to control the thickness of the pole strap. The laser thickness measurement sensor in the pole piece rolling equipment may have a loose position offset, resulting in the wrong measurement position.

D. HEALTH DIAGNOSIS STRATEGY OF LITHIUM BATTERY POLE DOUBLE ROLLING EQUIPMENT

We integrate the advantages and disadvantages of various single or fusion diagnosis methods and adopt the combined diagnosis method to improve the overall diagnostics accuracy of the equipment [40]. In this paper, the FEFDM of lithium battery pole double rolling equipment and the fuzzy set improved BP Neural Network health state evaluation method of lithium battery pole double rolling equipment are combined to achieve the overall comprehensive diagnosis ability of the equipment through its internal relationship. The frame structure of the health diagnosis method of lithium battery pole double rolling equipment is shown in Fig.5.

It can be seen from Fig.5 that this method takes the expert system theory as the basis of the overall diagnosis framework, and the reasoning part adopts two methods: fault diagnosis reasoning and health state evaluation. The functions of each module are as follows:

(1) Human-computer interaction module: Be responsible for the operation and control of the whole system, provide various information and operation interfaces of the equipment, and facilitate the management of the equipment.

(2) Knowledge acquisition module and machine learning module: It is used to update the fuzzy knowledge base of the diagnosis method and the database of pole piece double rolling equipment, to improve the intelligent ability of the equipment.

(3) Fuzzy knowledge base, database and model base: The knowledge base is called by the fault diagnosis inference engine—the database for managing and storing various equipment. The model base is responsible for the health evaluation of lithium battery pole double rolling equipment.

(4) Fault diagnosis reasoning and health status evaluation module: It is responsible for using the data collected by the system and fuzzy reasoning method to complete the fault diagnosis and health state evaluation of pole piece double roller equipment.

(5) Interpretation mechanism module: Be responsible for recording the process of fault diagnosis and health status evaluation, including the intermediate results of the diagnosis and evaluation process, so as to facilitate the equipment users to understand the diagnosis process.

III. RESEARCH ON FAULT DIAGNOSIS METHOD

A. COMPREHENSIVE DIAGNOSIS METHOD OF FEFDM

For the lithium battery pole double rolling equipment, due to the complexity of the equipment, many fault knowledge is fuzzy and cannot be accurately expressed. The fuzzy fault diagnosis method can fuzzily represent the uncertain knowledge in the complex equipment diagnosis object, reduce the number of rules set in the knowledge base, and improve the accuracy of fault diagnosis of the expert system [40]. The fuzzy comprehensive diagnosis method used in this paper first needs to diagnose each fault cause separately, and then comprehensively analyze all fault causes, which is mainly composed of the following five parts:

1) FAULT SYMPTOM SET

U is a collection of different signs that each fault may cause. On the other hand, fuzzy integrated diagnosis determines possible equipment signs after considering all the causes of the failure together.

2) FAULT CAUSES SET

V is a traditional set, and many of the failure causes in the set have fuzzy properties.

3) FAULT CAUSES WEIGHT SET

The failure causes of lithium battery pole double rolling equipment may be complex and diverse. To characterize each cause v_i for the importance of all fault causes, set the corresponding weight as a_i . Then we can get $A = \{a_1, a_2, \dots, a_n\}$. a_i can be normalized and meet the non-negative condition. Each element a_i in the weight is used to represent the degree of membership of v_i . It can be seen that the A is a fuzzy subset of V , and its expression is:

$$A = \frac{a_1}{v_1} + \frac{a_2}{v_2} + \dots + \frac{a_n}{v_n} \tag{1}$$

a : SINGLE FAULT CAUSES FUZZY DIAGNOSIS

If the membership degree of the i -th element u_i in the fault symptom set corresponding to the j -th element v_j in the fault

cause set is r_{ij} , then the result of v_i diagnosis can be expressed by fuzzy set:

$$R_i = \frac{r_{i1}}{u_1} + \frac{r_{i2}}{u_2} + \dots + \frac{r_{in}}{u_n} \quad (2)$$

R_i is a fuzzy subset of fault symptom set V , which can be recorded as $R_i = \{r_{i1}, r_{i2}, \dots, r_{in}\}$. R is the fuzzy relationship between U and V , which represents the subordinate relationship between fault symptom u_i and fault cause v_j .

b: FUZZY COMPREHENSIVE DIAGNOSIS OF FAULT CAUSES

The single fault causes fuzzy diagnosis of the possible symptoms of the diagnosis equipment must be inaccurate by analyzing a single fault cause. The accurate diagnosis results can be obtained only by comprehensively considering the influence of all fault causes. We can get:

$$B = A \cdot R = (a_1, a_2, \dots, a_m) \cdot \begin{pmatrix} r_{11} & \dots & r_{1n} \\ \vdots & \ddots & \vdots \\ r_{m1} & \dots & r_{mn} \end{pmatrix} = (b_1, b_2, \dots, b_m) \quad (3)$$

$$b_j = \bigvee_{i=1}^m (a_i \wedge r_{ij}), \quad j = 1, 2, \dots, n \quad (4)$$

b_j represents the membership degree of the diagnosis object to the j -th element in the fault cause symptom set after comprehensively considering the cross-influence of various fault causes.

B. DATABASE

Through the analysis of the fault types of double roller press equipment in the Section II, the following nine main fault symptom parameters affecting the regular operation of the equipment are summarized: $T, T', TO, F, F', Q, v, v'$ and P . According to their different characteristics, they are divided into different quantization levels. The level division and fault signal membership function are shown in Fig.6.

The relative error of the tension set in this paper is $\pm 10N$. The Z-type membership function is used as the left boundary and the anti-Z-type membership function is used as the right boundary. The triangular membership function is adopted data when the tension value is less than or greater than the grade. The degree of tension fluctuation largely reflects whether the tension control system is stable. Its calculation method calculates the standard deviation of the tension value, and the expression is shown in equation (5).

$$S = \sqrt{\frac{1}{n}[(T_1 - m)^2 + (T_2 - m)^2 + \dots + (T_n - m)^2]} \quad (5)$$

The Z-type membership function is the right boundary in the boundary selection, and the triangular membership function is used when the tension value is medium.

There is a linear relationship between the excitation current and torque of the magnetic particle brake, which takes the magnetic particle as the transmission medium to transmit the torque, and finally realizes the control of the torque. In this paper, the Z-type membership function is used as the left

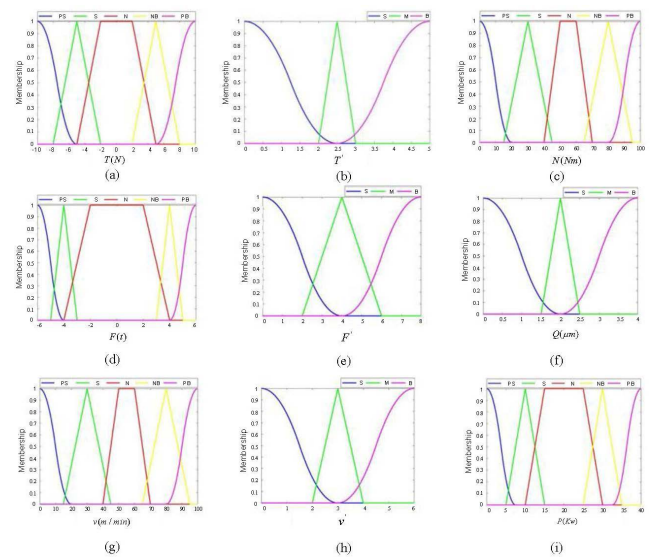


FIGURE 6. (a) Membership function of tension; (b) Membership function of tension fluctuation; (c) Membership function of magnetic particle brake torque; (d) Membership function of rolling pressure; (e) Membership function of rolling pressure fluctuation; (f) Membership function of polar strip thickness; (g) Membership function of rolling speed; (h) Membership function of rolling speed fluctuation; (i) Membership function of rolling motor operating power.

boundary, the anti-Z-type membership function is used as the right boundary, the trapezoidal membership function is used to keep the membership function stable when the grade is normal, and the triangular membership function is used when the grade is less than or greater than the grade.

The rolling pressure adopts the Z-type membership function as the left boundary and the anti-Z-type membership function as the right boundary. The fluctuation degree of rolling pressure can reflect the faults of the main rolling system of equipment. The Z-type membership function is also the left boundary in the boundary selection. The anti-Z-type membership function is used as the right boundary. The triangular membership function is used when the tension value is medium.

The thickness of the polar strip is mainly controlled by adjusting the roll gap adjustment system. The Z-type membership function is also the left boundary in the boundary selection. The anti-Z-type membership function is used as the right boundary. The triangular membership function is used when the tension value is medium.

The running power of the trolling motor is one of the fault-sensitive parameters of the double rolling equipment, and its running ability can reflect the working condition of the engine. The establishment method of its membership function is similar to the previous analysis, which is mainly composed of Z-type, anti-Z-type, triangular, and trapezoidal membership functions.

C. KNOWLEDGE BASE

Fuzzy knowledge is a fuzzy relation matrix established between fault cause and fault symptom fuzzy set. The value

TABLE 2. Fuzzy fault symptom set of pole piece double rolling equipment.

u_i	Fault symptom	u_i	Fault symptom
u_1	T	u_6	Q
u_2	T'	u_7	v
u_3	TO	u_8	v'
u_4	F	u_9	P
u_5	F'		

TABLE 3. Fuzzy fault reason set of pole piece double rolling equipment.

v_i	Cause of failure
v_1	The magnetic particle seal of the brake leaks due to magnetic particle leakage
v_2	The high temperature of the magnetic particle brake leads to a decrease in control accuracy
v_3	The tension sensor failure or position offset
v_4	Winding motor stuck
v_5	Rolling motor stuck
v_6	Jamming of the roll gap adjustment mechanism or failure of the thickness measurement sensor
v_7	Leakage of oil valve or seal in the pump
v_8	Roll deformation or wear
v_9	Unstable coupling or excessive motor load
v_{10}	The correction sensor failure or position offset

in the fuzzy relation matrix represents the closeness between the corresponding fault symptom and the fault cause [41], [42]. Table 2 summarizes the fuzzy fault symptom set $U = \{u_1, u_2, u_3, \dots, u_9\}$. Then, we classify and summarize the possible fault causes and fuzzy the fault cause set $V = \{v_1, v_2, v_3, \dots, v_{10}\}$, as shown in Table 3.

D. INFERENCE ENGINE

This paper selects the fuzzy comprehensive diagnosis method of fault causes. This method mainly calculates the fuzzy diagnosis index, and then selects the appropriate index processing method to obtain the diagnosis result. Considering the influence of multiple fault sign factors, the weighted matrix multiplication operation of U and R is carried out to derive the comprehensive diagnosis index, and then the maximum affiliation principle and the threshold principle are adopted to combine to obtain the diagnosis results.

Firstly, the corresponding membership degree of each fuzzy fault reason is calculated, and the fault reason with the most significant membership degree is taken as the candidate reasoning result, that is, $y_{vj} = \max(y_{v1}, y_{v2}, \dots, y_{v9})$. Then select the appropriate one through the threshold principle λ , finally, a reasonable diagnosis result is obtained. In this paper, the threshold is finally set according to the actual situation of the equipment $\lambda = 0.2$. To avoid the false alarm when the equipment has no-fault, the following simulation verification is carried out when the parameter level of each fault symptom of the equipment is normal. The reasoning results under the

condition of no fault of the simulation equipment are shown in Table 4.

IV. RESEARCH ON HEALTH STATUS EVALUATION METHOD

In this section, we propose the concept of health degree, divide the health state level through the fault state, and complete the mapping from health degree to health state level by using BP Neural Network and fuzzy set method, to conduct the research on the evaluation method of the health state of lithium battery pole double rolling equipment.

A. FAULT STATE HEALTH DIVISION

Through the study of health assessment methods, this section proposes the use of HD indicators to reflect the working condition of the equipment accurately. The HD function is defined by x_1, x_2, \dots, x_n , which can be recorded as:

$$HD = f'(x_1, x_2, \dots, x_n) \tag{6}$$

HD is an important concept, which has been studied in Engineering Technology for a long time. It is defined as $HD \in [0, 1]$. When HD is 1, it indicates that the equipment is very healthy, while when HD is 0, it indicates that the equipment has failed. The running state of the rolling mill is divided into fault state, sub-health state and health state, as shown in Table 5.

B. HEALTH MAPPING MODEL

Because this paper considers adding sub-health state to evaluate the running condition of the rolling mill, the three-phase fuzzy statistical method is adopted. Using the random interval theory of trisection method, three fuzzy subsets are established according to the division of health degree of pole piece double rolling equipment and the characteristics of improved BP Neural Network method: $\rightarrow A_1 = \text{“Fault”}$, $\rightarrow A_2 = \text{“Sub - health”}$, $\rightarrow A_3 = \text{“Health”}$. let $X \in [0, 1]$, and determine the division of X as:

$$X \Rightarrow \rightarrow A_1^* \cup \rightarrow A_2^* \cup \rightarrow A_3^* \tag{7}$$

Assuming that u and v are the boundary points of $\rightarrow A_1^*$ and $\rightarrow A_2^*$, $\rightarrow A_2^*$ and $\rightarrow A_3^*$ respectively, then (u,v) can be obtained from $(\rightarrow A_1^*, \rightarrow A_2^*, \rightarrow A_3^*)$. We take (u,v) as the observation value of a two-dimensional random vector for sampling. We can get the probability distribution of u and v , and finally get the membership function of $\rightarrow A_1$, $\rightarrow A_2$ and $\rightarrow A_3$.

Because $\rightarrow A_1, \rightarrow A_2, \rightarrow A_3 \in f'(X)$, (U,V) is random vector, and meet $P(U \leq V) = 1, \forall u, v \in X$, So (u,v) can determine the mapping:

$$f'(u, v) : X \rightarrow \{\rightarrow A_1, \rightarrow A_2, \rightarrow A_3\} \tag{8}$$

TABLE 4. Fault free simulation reasoning results.

Signal symptom	{N, S, N, N, N, S, S, N, S, S, N}	λ	Results
Fault membership	{1,1,1,1,1,1,1,1,1,1}	0.1	v_3
Comprehensive diagnostic index	$b_j(j = 1,2,\dots,n)$	0.15	v_3
Fault cause membership	{0.1, 0.05, 0.1, 0.05, 0.1, 0.1, 0.1, 0.05, 0,0}	0.2	No-fault

TABLE 5. Health status classification.

HD range	Health grade	State description
$0 \leq HD < 0.2$	Fault	Fault state
$0.2 < HD \leq 0.8$	Sub-health	Poor state
$0.8 \leq HD < 1$	Health	Normal state

get $\forall x \in X$, including:

$$f'(u, v)(x) \begin{cases} \rightarrow A_1, & 0 \leq x < u \\ \rightarrow A_2, & u \leq x < v \\ \rightarrow A_3, & v \leq x \leq 1 \end{cases} \quad (9)$$

If $P_U(t)$ and $P_V(t)$ are probability density functions corresponding to U and V , then:

$$\rightarrow A_1(x) = \int_x^1 P_U(t)dt \quad (10)$$

$$\rightarrow A_3(x) = \int_x^1 P_V(t)dt \quad (11)$$

$$\rightarrow A_2(x) = 1 - \rightarrow A_1(x) - \rightarrow A_3(x) \quad (12)$$

So, $V = \{v_1(\text{Fault}), v_2(\text{Sub-health}), v_3(\text{health})\}$, after quantizing, $V = (v_1, v_2, v_3)^T$ (where v_1, v_2, v_3 are non-negative coefficients).

Then the calculation formula of health degree can be obtained as:

$$HD = \rightarrow A \cdot V = (a_1, a_2, a_3) \cdot \begin{pmatrix} v_1 \\ v_2 \\ v_3 \end{pmatrix} = v_1 a_1 + v_2 a_2 + v_3 a_3 \quad (13)$$

In the formula (13), $\rightarrow A$ is the corresponding membership degree of the health state fuzzy set calculated by BP Neural Network; v_1, v_2, v_3 is a positive coefficient.

C. OPTIMIZATION OF NETWORK TOPOLOGY STRUCTURE

The determination of input layer nodes should consider the characteristics of pole piece double rolling equipment and the correlation between each parameter. Integrating the fault symptom analysis and principal component analysis in Section III, the input variables are determined as $T, TO, F, Q,$

TABLE 6. Variable definition of neural network.

Node location	Variables	Definition
Input layer	T	I_1
	TO	I_2
	F	I_3
	Q	I_4
	v	I_5
	P	I_6
Output layer	a_1	O_1
	a_2	O_2
	a_3	O_3

V and P . The description of BP Neural Network input nodes is shown in Table 6.

Although the number of hidden layers can enhance the network performance, it will increase the training time. Therefore, this paper adopts the three-layer network structure of a single hidden layer. BP Neural Networks have the best number of hidden layer node s^* , When the number of hidden layer nodes $s > s^*$, it is easy to appear ‘‘overfitting’’ in the process of training, When the number of hidden layer nodes $s < s^*$, the inductive learning ability of neural network will decline. The commonly used empirical formula is:

$$s = 2 \sum_{i=1}^6 I_i + 1 \quad (14)$$

$$s = \sqrt{\sum_{i=1}^6 I_i + \sum_{i=1}^3 O_i} + a, \quad a \in [1, 10] \quad (15)$$

To improve the network performance, we use the measurement method of percentage accuracy to verify the prediction performance of neural networks with different hidden layers. Its main performance indicators are defined as:

$$Accuracy_i = (1 - |HD_i - HD_i|) \times 100\%, \quad i = 1, 2, \dots, n \quad (16)$$

$$\overline{Accuracy} = \frac{1}{n} \sum_{i=1}^n Accuracy_i, \quad i = 1, 2, \dots, n \quad (17)$$

where, $Accuracy_i$ is the accuracy of each sample, $\overline{Accuracy}$ is the average accuracy of all models, n is the number of pieces. In this test, $n = 200$, the expected error is 0.01, and the training times are 800. The average accuracy of

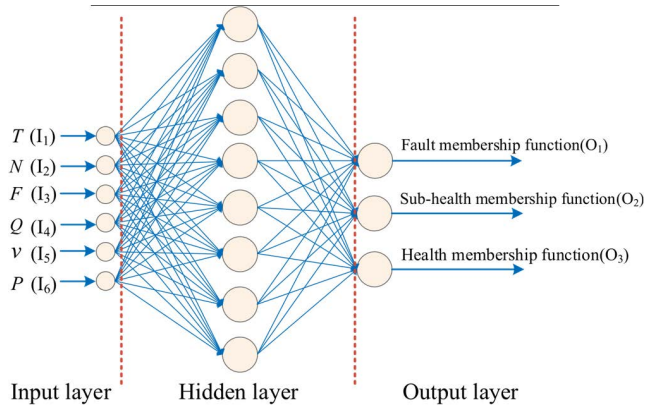


FIGURE 7. Neural network structure of pole piece double rolling equipment.

TABLE 7. Average accuracy of the neural network corresponding to different numbers of hidden layer nodes.

Number of hidden layer nodes	Accuracy
5	88.97%
6	90.36%
7	92.42%
8	95.23%
9	93.85%
10	91.14%

TABLE 8. Hyperparameters for the experiments.

Layers	Design Details	Parameters Setting
BP Neural Network	Number of input layers: 6	Batch size: 20
	Number of neurons: 8	Epochs: 60
	Sampling number: 4	Learning rate: 0.1
	Expected error: 0.01	Learning times: 1000
		Bias: 0 Weights: (-1,1)

the neural network corresponding to the different number of nodes is shown in Table 7. Compared with the number of other hidden layer nodes, when the number of nodes is 8, the value *Accuracy* is the largest, so the extension structure of this neural network is 6-8-3, and the design of the BP neural network is shown the Fig.7

The BP Neural Network is trained using the *Sigmoid* algorithm for supervised training, and the model is prepared using a small batch sampling method. The model’s hyperparameters, such as learning rate and expectation error, are continuously updated using the gradient descent algorithm, as shown in Table 8.

D. DATA ACQUISITION AND PREPROCESSING

1) DATA ACQUISITION

From the previous chapter, we determined the variable properties of the final input network. We have installed corresponding sensors on the mechanical equipment to obtain accurate on-site real-time data. Among them, I_5 and I_6 are

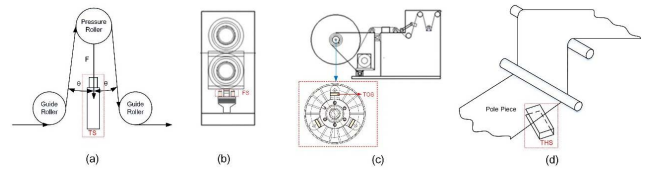


FIGURE 8. (a) Tension sensor installation location; (b) Pressure sensor installation location; (c) Torque sensor mounting position; (d) Thickness sensor installation location.

directly obtained from the inverter and the rolling motor without installing sensors. We installed sensors on the pressure roller, magnetic powder brake, hydraulic system, and pole piece belt, respectively, to collect the data of I_1 - I_4 . The specific installation location is shown in Fig.8, and the meanings of the relevant characters are shown in Table 1.

The TS is installed between the two guide rollers. To ensure tension stability, the θ between the TS and the pole strip on both sides should be kept the same. The specific installation position is shown in Fig.8(a).

The hydraulic system generates the rolling pressure, so it is only necessary to install the FS between the hydraulic system and the roll to obtain the rolling pressure precisely. The specific installation position is shown in Fig.8(b). We installed FS on each side of the rolls, and the final pressure value is the arithmetic average of the two FSs, eliminating the effect of body vibration on FS.

The magnetic powder brake is installed in the winding and unwinding system, and its internal structure and TOS installation position are shown in Fig.8(c). The magnetic powder brake torque control can affect the tension of the winding and unwinding rolls. Changing the tension force inside the magnetic powder brake can shrink or stretch the pole strip. We have arranged three TOS inside the magnetic powder brake, which can collect the tension force in three directions.

We install THS at the end of the winding mechanism, THS is a photoelectric sensor, which can be used to measure the thickness of the pole piece.

The sample data of pole piece double rolling equipment are selected from three states: normal operation, sub-health operation and fault operation. Table 9 shows part of the original data.

2) EKF

The lithium battery pole mill is a nonlinear mechanical system, so we use nonlinear data digital filtering algorithm. The EKF is a linearization of a nonlinear function in the form of a Taylor series expansion that preserves the first order term to achieve linearization of the nonlinear function [43], [44]. It replaces the state transfer matrix in the Kalman filter equation with the Jacobi matrix. It then calculates the state estimates and variance of the system using the Kalman filter algorithm as a framework [45]. EKF can effectively solve the nonlinear state estimation problem [46].

TABLE 9. Part of the original data.

$T(N)$	$TO(Nm)$	$F(t)$	$Q(mm)$	$v(m/min)$	$P(KW)$
120.7	60.7	61.6	0.2093	50.4	20.2
118.9	59.9	60.8	0.2026	49.3	19.4
121.1	60.1	59.3	0.1984	50.1	20.1
123.3	60.1	60.4	0.2093	51.1	20.7
117.4	61.4	57.5	0.2104	52.3	21.4
121.7	61.4	61.4	0.2103	51.4	21.8
122.2	63.3	63.7	0.1997	53.7	23.3
124.6	62.6	59.6	0.1842	52.5	22.5
123.5	61.5	62.4	0.2120	50.4	19.2
124.6	61.6	64.8	0.2285	49.5	21.6
124.1	64.1	63.2	0.2222	48.7	24.1
122.4	64.4	62.7	0.2094	53.4	22.4
120.1	60.2	63.1	0.2178	50.2	20.1
118.6	60.6	60.9	0.2108	50.5	21.5
117.8	60.6	62.2	0.2034	51.8	20.2
119.2	64.3	63.8	0.1929	54.3	24.3
121.5	64.5	56.3	0.2012	54.4	24.1
121.6	61.6	62.5	0.2106	51.5	21.2
122.6	60.6	61.5	0.2008	49.5	20.2
121.4	61.4	62.4	0.2082	51.6	19.4
120.6	62.6	59.1	0.1982	52.5	22.2
119.5	61.5	63.6	0.1920	51.4	21.1
118.6	61.6	62.8	0.2026	50.2	21.2
120.1	64.1	60.7	0.2021	54.3	24.1
123.4	64.4	58.6	0.2205	54.4	24.4
125.7	62.7	56.8	0.2159	52.7	22.7

We consider the lithium battery pole mill operation data contains Gaussian white noise, the state space of the nonlinear stochastic system is defined as, the meaning of the variables in the state space equation is shown in Table 1:

$$\begin{cases} x_{k+1} = f(x_k) + \omega_k \\ z_k = h(x_k) + c_k \end{cases} \quad (18)$$

We use a first-order Taylor function to implement the nonlinear running parameters for linearization. We perform a first-order Tait expansion of the nonlinear function $f(x_k)$ at $\hat{x}_{k|k}$:

$$f(x_k) = f(\hat{x}_{k|k}) + \frac{\partial f}{\partial x_k} \Big|_{x_k = \hat{x}_{k|k}} (x_k - \hat{x}_{k|k}) + o(x_k - \hat{x}_{k|k}) \quad (19)$$

where $o(x_k - \hat{x}_{k|k})$ is a higher order term, we define $\frac{\partial f}{\partial x_k} \Big|_{x_k = \hat{x}_{k|k}} = F_k$. Neglecting the higher order terms [47], the equation of state simplifies to:

$$x_{k+1} = f(\hat{x}_{k|k}) + F_k(x_k - \hat{x}_{k|k}) + \omega_k \quad (20)$$

Further, we can obtain the one-step state prediction and the one-step state prediction covariance for the nonlinear

function:

$$\hat{x}_{k+1|k} = E[f(\hat{x}_{k|k}) + F_k(x_k - \hat{x}_{k|k}) + \omega_k] \quad (21)$$

$$\begin{aligned} P_{k+1|k} &= E[(x_{k+1} - \hat{x}_{k+1|k})(x_{k+1} - \hat{x}_{k+1|k})^T] \\ &= F_k P_{k|k} F_k^T + Q_k \end{aligned} \quad (22)$$

After that, we expand the nonlinear function $h(\cdot)$ in a first-order Taylor expansion at the one-step state prediction $\hat{x}_{k+1|k}$ [48]:

$$\begin{aligned} h(x_{k+1}) &= h(\hat{x}_{k+1|k}) + \frac{\partial h}{\partial x_{k+1}} \Big|_{x_{k+1} = \hat{x}_{k+1|k}} (x_{k+1} - \hat{x}_{k+1|k}) \\ &\quad + o(x_{k+1} - \hat{x}_{k+1|k}) \end{aligned} \quad (23)$$

where $o(x_{k+1} - \hat{x}_{k+1|k})$ is a higher order term, we define $\frac{\partial h}{\partial x_{k+1}} \Big|_{x_{k+1} = \hat{x}_{k+1|k}} = H_{k+1}$. Neglecting the higher order terms, the observation equation simplifies to:

$$z_{k+1} = h(\hat{x}_{k+1|k}) + H_{k+1}(x_{k+1} - \hat{x}_{k+1|k}) + c_{k+1} \quad (24)$$

$$\begin{aligned} P_{z_{k+1}|k} &= E[(z_{k+1} - \hat{z}_{k+1|k})(z_{k+1} - \hat{z}_{k+1|k})^T] \\ &= H_{k+1} P_{k+1|k} H_{k+1}^T + R_{k+1} \end{aligned} \quad (25)$$

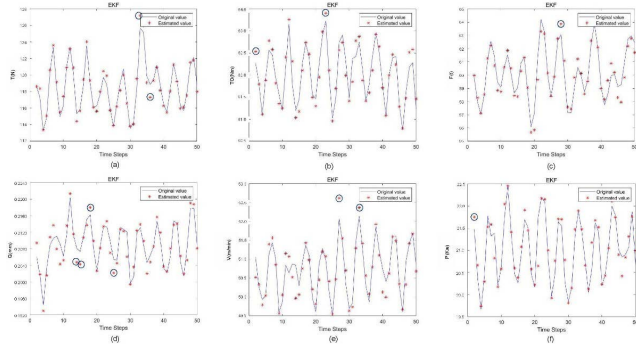


FIGURE 9. (a) Tension data EKF filtering results; (b) Torque data EKF filtering results; (c) Rolling force data EKF filtering results; (d) Thickness data EKF filtering results; (e) Rolling speed data EKF filtering results; (f) Motor power data EKF filtering results.

$$P_{xz,k+1|k} = E[(x_{k+1} - \hat{x}_{k+1|k})(z_{k+1} - \hat{z}_{k+1|k})^T] \\ = P_{k+1|k} H_{k+1}^T \quad (26)$$

Finally, we must obtain the state gain matrix, which is used to calculate the state estimation covariance matrix at the time [49]. The state gain matrix is:

$$K_{k+1} = P_{xz,k+1|k} (P_{zz,k+1|k})^{-1} \\ = P_{k+1|k} H_{k+1}^T (H_{k+1} P_{k+1|k} H_{k+1}^T + R_{k+1})^{-1} \quad (27)$$

State estimate at time $k + 1$:

$$\hat{x}_{k+1|k+1} = \hat{x}_{k+1|k} + K_{k+1}(z_{k+1} - \hat{z}_{k+1|k}) \quad (28)$$

State estimation error covariance matrix:

$$P_{k+1|k+1} = E[(x_{k+1} - \hat{x}_{k+1|k+1})(x_{k+1} - \hat{x}_{k+1|k+1})^T] \quad (29)$$

The data after filtering are shown in Fig.9. We set a fixed accuracy for each variable present in the experiment to ensure that the correct estimation information is extracted [50]. As shown in Fig.9(a), the initial value of tension is set to 117N. In the 0 moment of $x_{(0|0)}$ and $P_{(0|0)}$ are 117 and 1, respectively, the use of k moment tension is expected to the moment of tension, at this time, $P_{k+1|k} = 0.2$, $K_{k+1} = 0.8005$, according to which the next moment of tension value of 116N. In the same way, according to the set parameters, update $P_{k+1|k}$ and K_{k+1} at time k of other parameters, and update the data at the next time [51].

In addition, as shown in Fig.9(a)-(f), we collect the time points where the deviation between the original data and the predicted data is large, and we find that the time points with large deviation are concentrated in the middle time step. By calculation, the mean squared error of the EKF-based digital filtering method is 1.21, and the prediction error is low.

3) EXPERIMENTAL SIMULATION

There are 1200 sets of sample data of lithium battery pole double rolling equipment, of which 900 sets are selected for training and the remaining 300 sets are selected for testing.

Test the remaining 300 groups of samples, including 100 groups of data of health status, sub-health status and

fault status. After the membership degrees of the corresponding three sets are obtained through improved neural network training, the corresponding health degree ($V = (v_1, v_2, v_3)^T = (1.0, 0.5, 0)^T$) is further calculated by equation (13). The membership and health of 18 groups of test data and the corresponding health status of pole piece double rolling equipment are listed here. 6 groups are selected for each status, as shown in Table 10 below.

It can be seen from Table 10 that when the pole piece double rolling equipment is in healthy operation, the health degree of the collected data is between 0.8-1, and the ‘‘Health’’ evaluation result is consistent with the actual production state of the equipment. When the pole piece double rolling equipment is in sub-health operation, the health degree of the collected data is almost between 0.2 and 0.8. Although one of them is rated as ‘‘Health,’’ its health degree is also very close to the critical value of 0.8, and the evaluation result of ‘‘Sub-health’’ is consistent with the actual production state of the equipment. When the pole piece double roller press equipment is in fault operation, the health evaluation of the collected data is between 0-0.2, and the evaluation result of ‘‘Fault’’ is consistent with the actual production state of the equipment. It can be seen that the establishment of the health status evaluation method is basically in line with the actual situation, and the evaluation of the operation status of lithium battery pole double rolling equipment is reasonable.

V. EXPERIMENT

This section applies the health diagnosis method to the lithium battery pole piece double rolling equipment. During the operation of the pole piece double rolling equipment, the equipment state is detected, the inference engine of the fault diagnosis method is used to diagnose the equipment fault, and the health state of the equipment is evaluated by using the health theory of the health state evaluation method.

A. EXPERIMENT I

During the working process of lithium battery double rolling equipment, the tension value will be set in advance according to the specific production requirements. In this paper, the tension value of 120 N is taken as the set value. The upper limit of tension is 130 N and the lower limit is 110 N. After the equipment operates continuously for some time, the tension sensor interferes artificially, and the fault alarm function is triggered at this time. The human-computer interaction interface automatically jumps to the fault diagnosis interface, as shown in Fig.10.

As shown in Fig.10, the fault diagnosis interface has diagnosed and made decisions on the results. It is determined that the fault location is the winding control system, and the fault reason is the fault or offset of the tension sensor. Two fault decisions are given: replacing the tension sensor and checking the winding motor, consistent with the experimental human intervention results. Observe the tension curve interface of the real-time monitoring interface, as shown in Fig.11.

TABLE 10. Simulation results of health status evaluation of pole piece double rolling equipment.

Working condition	Health set	Sub-health set	Fault set	HD	Operation Status
Health operation status	0.7845	0.2143	0.0124	0.8917	Health
	0.7932	0.2035	0.0086	0.8950	Health
	0.8057	0.1946	0.0123	0.9030	Health
	0.7834	0.2265	0.0095	0.8967	Health
	0.8176	0.1774	0.0107	0.9063	Health
	0.8097	0.1895	0.0137	0.9045	Health
Sub-health operation state	0.6037	0.4012	0.0021	0.8043	Health
	0.5867	0.4124	0.0018	0.7929	Sub-health
	0.5913	0.4055	0.0015	0.7941	Sub-health
	0.5956	0.4036	0.0024	0.7974	Sub-health
	0.5889	0.4159	0.0019	0.7969	Sub-health
	0.5924	0.4052	0.0023	0.7950	Sub-health
Fault operation status	0.0095	0	0.9971	0.0095	Fault
	0.0145	0	0.9714	0.0145	Fault
	0.0647	0	0.9345	0.0647	Fault
	0.0043	0	0.9823	0.0043	Fault
	0.0034	0	0.9296	0.0034	Fault
	0.0279	0	0.9942	0.0279	Fault

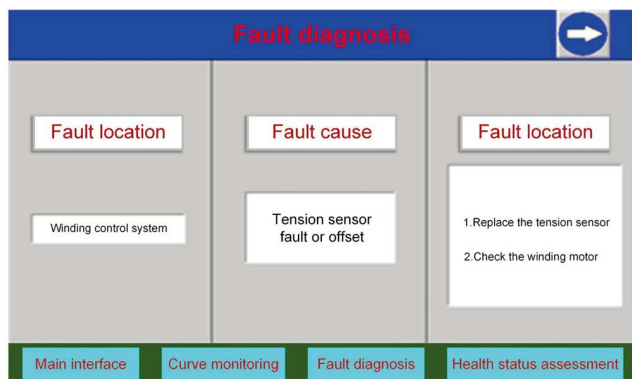


FIGURE 10. Fault diagnosis interface.

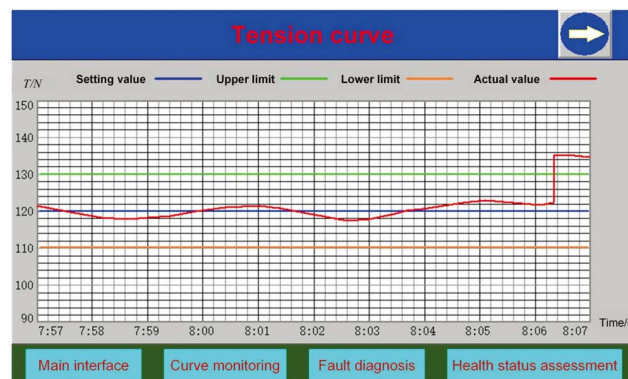


FIGURE 11. Tension curve interface.

Observing the actual value curve of tension shows that when the equipment is in normal operation from 7:57 to 8:06, the fluctuation degree of tension value is relatively stable and stable within 5%. When the tension value suddenly rises after 8:06, the tension value is 133.16N, triggering the alarm. According to the fault characteristic parameter signal, the fuzzy fault symptom set at this time is obtained as:

$$U = \{0.9257, 0.8635, 0.9813, 1, 1, 1, 1, 1, 1\}$$

According to the comprehensive diagnosis index formula, the weight matrix method is used for fuzzy operation. The membership degree corresponding to each fault cause v_j in the fuzzy fault cause set V is calculated. The calculation results

are as follows:

$$Y = \{0.3581, 0.15, 0.8562, 0.5874, 0.1, 0.15, 0.05, 0.1, 0.1, 0.2\}$$

The final result of fuzzy reasoning is $y_{v3} = 0.8562$, and the corresponding fault cause is v_3 . Therefore, the fault reason in the component interface of fuzzy fault diagnosis is the fault or offset of the tension sensor, which is the result of the fuzzy diagnosis.

B. EXPERIMENT II

The no-load test shall be carried out before the lithium battery double roller equipment starts operation. In this experiment, the rolling speed is preset to 40 m / min. After the equipment

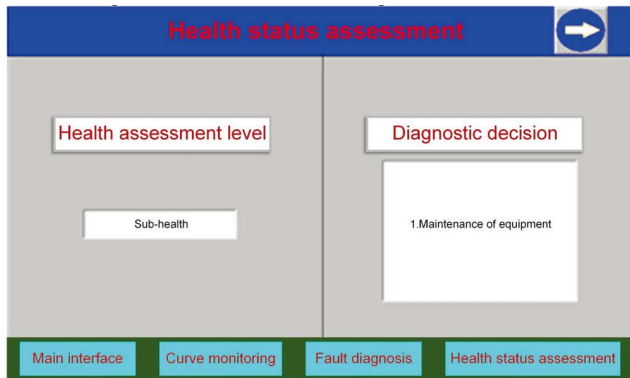


FIGURE 12. Health status assessment interface.

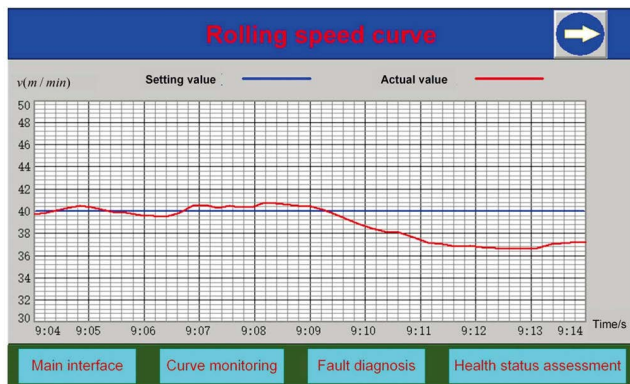


FIGURE 13. Rolling speed curve interface.

TABLE 11. Health status assessment results.

Health set	Sub-health set	Fault set	HD	Operation Status
0.5853	0.4238	0.0012	0.7972	Sub-health

operates stably for a period of time, in order to reduce the motor speed and reduce the rolling rate, the equipment will give an alarm. The health status evaluation interface is shown in Fig.12. It can be seen from Fig.12 that the health status evaluation interface has evaluated the health level and made a decision. It is determined that the pole piece double rolling equipment is in sub-health status. The rolling speed curve interface of the real-time monitoring interface is shown in Fig. 13.

By observing the rolling speed curve, it can be seen that the equipment is in normal operation from 9:04 to 9:09. At this time, the fluctuation degree of rolling speed is relatively stable and stable within 5%. After 9:09, the rolling speed begins to decline rapidly. At this time, the rolling speed is 36.57m/min, triggering the sub-health state alarm. At this time, the equipment health evaluation results are shown in Table 11. The experiment shows that the rolling mill operation state evaluation is accurate and suitable for an industrial site.

VI. CONCLUSION

This paper mainly introduces an intelligent health diagnosis method of battery pole double rolling equipment based on the Hybrid BP Neural Network Expert System. This paper analyzes the research status of health diagnosis methods of battery pole double rolling equipment. It summarizes the development trend and shortcomings of health diagnosis methods of battery pole double rolling equipment. In this paper, the rolling process and the control elements of the equipment are analyzed in detail, and the failure of the lithium battery pole double rolling equipment is summarized. At the same time, a fault diagnosis method of double roller press equipment based on FEFDM is proposed in this paper. Combining fuzzy theory with expert system theory, the core part of fuzzy fault diagnosis expert system of pole piece double rolling equipment is analyzed in detail. Finally, based on the original fault diagnosis method, this paper introduces the concept of a health degree. It puts forward a health state evaluation method of lithium battery pole double rolling equipment based on a fuzzy improved neural network.

Aiming at the problem of complex and uncertain fault causes of double roller press equipment, combined with mathematical statistics and expert experience technology, the problem that it is challenging to establish expression rules for fuzzy issues in an expert system knowledge base is effectively solved. The fuzzy reasoning method is used to improve the reasoning mechanism of the expert system, realize the fuzzy reasoning of the fault of the lithium battery pole double rolling equipment, and establish the fault diagnosis method of the fuzzy expert system of the lithium battery pole double rolling equipment.

Combined with the actual situation in which the equipment fault state is fuzzy, this paper puts forward the concept of health degree and divides the equipment health state. Secondly, after analyzing the nonlinear characteristics of the double roller equipment system, a health evaluation method using fuzzy set optimization BP neural network to complete the health mapping is proposed. We calculate the membership degree corresponding to each fuzzy set, establish the mapping relationship between membership degree and health degree, realize the quantitative evaluation method of equipment health state, and establish the health state evaluation model of lithium battery pole double rolling equipment.

In the future, the improvement of the intelligent health diagnosis method of battery pole double rolling equipment driven by the Hybrid BP Neural Network Expert System is mainly reflected in the following aspects:

(1) To speed up the network training, this paper only lists some important fault factors. It is challenging to locate and diagnose unknown faults in equipment production accurately. The fault types of pole piece double roller equipment can be continuously improved and supplemented in the future.

(2) The fuzzy knowledge base needs to be supplemented with the accumulation of the number of fault cases diagnosed and the gradual supplement of professional knowledge.

Professional technicians must modify every time, which is not conducive to the maintenance and upgrading of a fuzzy expert system. Here, the more advanced self-learning adaptive algorithm can be introduced to optimize combined with the expert system.

(3) In the future, this health diagnosis method can be combined with remote monitoring technology to realize remote health diagnosis of pole piece double roller equipment, which is helpful to upgrade and maintain the system. Especially in today's epidemic background, remote diagnosis is more important.

REFERENCES

- [1] S. Jingna, X. Wenjie, H. Huagui, Y. Zhenge, and L. Jinrui, "Research progress of lithium battery pole piece rolling technology," *China Metall.*, vol. 31, no. 5, pp. 12–18, 2021.
- [2] S. King and N. J. Boxall, "Lithium battery recycling in Australia: Defining the status and identifying opportunities for the development of a new industry," *J. Cleaner Prod.*, vol. 215, pp. 1279–1287, Apr. 2019.
- [3] P. Rodríguez-Pajarón, A. Hernández, and J. V. Milanovic, "Probabilistic assessment of the impact of electric vehicles and nonlinear loads on power quality in residential networks," *Int. J. Electr. Power Energy Syst.*, vol. 129, pp. 106807–106820, Jul. 2021.
- [4] D. Qiao, G. Wang, T. Gao, B. Wen, and T. Dai, "Potential impact of the end-of-life batteries recycling of electric vehicles on lithium demand in China: 2010–2050," *Sci. Total Environ.*, vol. 764, Apr. 2021, Art. no. 142835.
- [5] S. Dingyu and G. Lin, "Design of power lithium-ion battery pole piece rolling mill control system based on STM32," *Instrum. Technol. Sensors*, no. 6, pp. 83–86 and 91, 2020.
- [6] S. S. Voronin, V. R. Gasiyarov, and E. A. Maklakova, "Modelling of the hydraulic work roll bending control system of the plate rolling mill," in *Proc. IEEE Conf. Russian Young Res. Electr. Electron. Eng.*, Feb. 2017, pp. 1060–1063.
- [7] Y.-F. Ji, D.-H. Zhang, S.-Z. Chen, J. Sun, X. Li, and H.-S. Di, "Algorithm design and application of novel GM-AGC based on mill stretch characteristic curve," *J. Central South Univ.*, vol. 21, no. 3, pp. 942–947, Mar. 2014.
- [8] Z. Hancheng, "Research on embedded control system of lithium battery pole piece rolling mill," Hebei Univ. Technol., Tianjin, China, 2018, doi: 10.27105/d.cnki.ghbgu.2018.000085.
- [9] H. Lan, W. Jinglin, L. Zeli, and S. Yong, "Key technologies and research paths of integrated system health management," *Aviation Sci. Technol.*, vol. 31, no. 7, pp. 12–17, 2020.
- [10] H. Henaio, G.-A. Capolino, M. Fernandez-Cabanias, F. Filippetti, C. Bruzzese, E. Strangas, R. Pusca, J. Estima, M. Riera-Guasp, and S. Hedayati-Kia, "Trends in fault diagnosis for electrical machines: A review of diagnostic techniques," *IEEE Ind. Electron. Mag.*, vol. 8, no. 2, pp. 31–42, Jun. 2014.
- [11] L. Yang, J. Wang, G. Zhang, and Z. Ding, "An expert system reasoning machine based on the combination of fault tree and generalized regression neural network," in *Proc. 12th World Congr. Intell. Control Autom. (WCICA)*, Jun. 2016, pp. 1303–1306.
- [12] Y. Shasha, "Research on fault diagnosis expert system of DC charging pile based on fault tree," Beijing Jiaotong Univ., Beijing, China, 2019.
- [13] L. Li and S. X. Ding, "Optimal detection schemes for multiplicative faults in uncertain systems with application to rolling mill processes," *IEEE Trans. Control Syst. Technol.*, vol. 28, no. 6, pp. 2432–2444, Nov. 2020.
- [14] M. He and D. He, "Deep learning based approach for bearing fault diagnosis," *IEEE Trans. Ind. Appl.*, vol. 53, no. 3, pp. 3057–3065, May/Jun. 2017, doi: 10.1109/TIA.2017.2661250.
- [15] H. Rui, "Early fault diagnosis of key parts of rolling mill based on cross-correlation energy ratio entropy and BiGRU-GRU," *Comput. Meas. Control*, vol. 30, no. 2, pp. 95–102, 2022.
- [16] C. Zhao, J. Sun, S. Lin, and Y. Peng, "Fault diagnosis method for rolling mill multi row bearings based on AMVMD-MC1DCNN under unbalanced dataset," *Sensors*, vol. 21, no. 16, p. 5494, 2021.
- [17] H. Luo, K. Li, O. Kaynak, S. Yin, M. Huo, and H. Zhao, "A robust data-driven fault detection approach for rolling mills with unknown roll eccentricity," *IEEE Trans. Control Syst. Technol.*, vol. 28, no. 6, pp. 2641–2648, Nov. 2020.
- [18] X. Hua, Y. Jin, T. Zhihui, and D. Jianqing, "Fault diagnosis of main drive shaft fracture of hot rolling vertical rolling mill," *Metall. Equip.*, pp. 66–67 and 98, 2021.
- [19] X. Dongmei, "On-line monitoring and fault diagnosis analysis of bearing vibration of high-speed wire rolling mill," *Mod. Manuf. Technol. Equip.*, no. 3, p. 154 and 156, 2018.
- [20] X. Debing, "Research on fault diagnosis of AGC hydraulic system of rolling mill," *Metall. Equip.*, no. 2, pp. 22–25, 2021.
- [21] H. Zhu, "Machine-learning-based mechanical fault diagnosis method," *Adv. Mater. Res.*, vols. 1044–1045, pp. 798–800, Oct. 2014.
- [22] J.-R. Ruiz-Sarmiento, J. Monroy, F.-A. Moreno, C. Galindo, J.-M. Bonelo, and J. Gonzalez-Jimenez, "A predictive model for the maintenance of industrial machinery in the context of industry 4.0," *Eng. Appl. Artif. Intell.*, vol. 87, Jan. 2020, Art. no. 103289.
- [23] R. Jiao, K. Peng, and J. Dong, "Remaining useful life prediction for a roller in a hot strip mill based on deep recurrent neural networks," *IEEE/CAA J. Autom. Sinica*, vol. 8, no. 7, pp. 1345–1354, Jul. 2021.
- [24] L. Xiangqian, "Research on key technologies of complex equipment failure prediction and health management," Beijing Inst. Technol., Beijing, China, 2014.
- [25] F. Wengpeng and L. Weigang, "Application of down-pressing big data mining in health diagnosis of four-high rolling mill," *Metall. Automat.*, no. 10, pp. 1–8, 2020.
- [26] Z. Qiao and X. Shu, "Coupled neurons with multi-objective optimization benefit incipient fault identification of machinery," *Chaos, Solitons Fractals*, vol. 145, Apr. 2021, Art. no. 110813, doi: 10.1016/j.chaos.2021.110813.
- [27] X. Xiaoyun and L. Hu, "Research on rolling bearing health warning of CNC machine tools based on self-learning SOM and ARMA algorithm," *Small Microcomput. Syst.*, vol. 40, no. 1, pp. 215–220, 2019.
- [28] S. Lijie, "Research on strip thickness optimization control and rolling process health status assessment method," Dalian Univ. Technol., Dalian, China, 2018.
- [29] W. Xin, "Research on health management technology in equipment system," Xidian Univ., Xi'an, China, 2018.
- [30] F. Yin, "Discrete model predictive control scheme for an integrated gauge-looper control system in a tandem hot strip mill," *IEEE Access*, vol. 8, pp. 73972–73985, 2020.
- [31] Z. Y. Zhang and X. Yi, "Design and implementation of the intelligent controller for electric ship," *J. Phys., Conf. Ser.*, vol. 1639, no. 1, Oct. 2020, Art. no. 012002.
- [32] M. Songke, "Lithium-ion battery production process and its development prospect," *Chem. Times*, vol. 33, no. 9, pp. 29–32, 2019.
- [33] R. J. Brodd and C. Helou, "Cost comparison of producing high-performance Li-ion batteries in the U.S. and in China," *J. Power Sources*, vol. 231, pp. 293–300, Jun. 2013.
- [34] T. Kornas, E. Knak, R. Daub, U. Bühner, C. Lienemann, H. Heimes, A. Kampker, S. Thiede, and C. Herrmann, "A multivariate KPI-based method for quality assurance in lithium-ion-battery production," *Proc. CIRP*, vol. 81, pp. 75–80, Jan. 2019.
- [35] X. Yanjun, Q. Hao, Z. Zhou, P. Kai, M. Zhaozong, and Z. Xuehui, "Detection and identification of surface defects of lithium battery pole piece rolling mill rolls," *J. Electron. Meas. Instrum.*, vol. 33, no. 10, pp. 148–156, 2019.
- [36] X. Yanjun, Q. Hao, W. Zhao, and X. Yanchun, "Analysis of the influence of rollers on the thickness consistency of battery pole pieces," *J. Hefei Univ. Technol. (Natural Sci. Ed.)*, vol. 42, no. 11, pp. 1490–1497, 2019.
- [37] C. Shengli, H. Anrui, X. Zhirang, S. Jian, and L. Yang, "Real-time comprehensive crown prediction and application of roll system in a rolling unit," *Chin. J. Mech. Eng.*, vol. 53, no. 2, pp. 61–66, 2017.
- [38] X. Liu, X.-H. Liu, M. Song, X.-K. Sun, and L.-Z. Liu, "Theoretical analysis of minimum metal foil thickness achievable by asymmetric rolling with fixed identical roll diameters," *Trans. Nonferrous Met. Soc. China*, vol. 26, no. 2, pp. 501–507, Feb. 2016.
- [39] W. Nenghe et al., "Simulation analysis of the drying process of negative electrode sheet coating for lithium batteries," *Power Technol.*, vol. 44, no. 1, pp. 42–44, 2020.
- [40] M. Altaf, T. Akram, M. A. Khan, M. Iqbal, M. M. I. Ch, and C.-H. Hsu, "A new statistical features based approach for bearing fault diagnosis using vibration signals," *Sensors*, vol. 22, no. 5, p. 2012, Mar. 2022.
- [41] M. Schmid, E. Gebauer, C. Hanzl, and C. Endisch, "Active model-based fault diagnosis in reconfigurable battery systems," *IEEE Trans. Power Electron.*, vol. 36, no. 3, pp. 2584–2597, Mar. 2021, doi: 10.1109/TPEL.2020.3012964.

- [42] X. Xu, D. Cao, Y. Zhou, and J. Gao, "Application of neural network algorithm in fault diagnosis of mechanical intelligence," *Mech. Syst. Signal Process.*, vol. 141, Jul. 2020, Art. no. 106625, doi: 10.1016/j.ymssp.2020.106625.
- [43] M. Fernandes, J. M. Corchado, and G. Marreiros, "Machine learning techniques applied to mechanical fault diagnosis and fault prognosis in the context of real industrial manufacturing use-cases: A systematic literature review," *Appl. Intell.*, 2022, doi: 10.1007/s10489-022-03344-3.
- [44] T. M. Thompkins, D.-I. Kim, P. Stone, and Y.-J. Shin, "Rolling mill cyclo-converter condition assessment by harmonic current via time-frequency signature," *IEEE Trans. Ind. Informat.*, vol. 14, no. 10, pp. 4376–4384, Oct. 2018.
- [45] C. Zhengxin, "Motor parameter estimation based on improved Kalman filter algorithm," Nanjing Univ. Posts Telecommun., Nanjing, China, 2021.
- [46] C. Fan, Z. Xinggan, and B. Yechao, "Lateral velocity estimation based on extended Kalman filter," *J. Nanjing Univ., Natural Sci.*, vol. 57, no. 5, pp. 864–869, 2021, doi: 10.13232/j.cnki.jnju.2021.05.017.
- [47] F. Jiayu, X. Jing, C. Nan, and Y. Yongjun, "Online estimation of SOC of electric vehicle lithium battery based on modified covariance extended Kalman filter," *J. Southeast Univ.*, vol. 36, no. 2, pp. 128–137, 2020.
- [48] C. Yukun, S. Xicai, and L. Zhigang, "Research on Kalman-filter based multisensor data fusion," *J. Syst. Eng. Electron.*, vol. 18, pp. 497–502, 2007, doi: 10.1016/S1004-4132(07)60119-4.
- [49] C. Jiang, S. Wang, B. Wu, C. Fernandez, X. Xiong, and J. Coffie-Ken, "A state-of-charge estimation method of the power lithium-ion battery in complex conditions based on adaptive square root extended Kalman filter," *Energy*, vol. 219, Mar. 2021, Art. no. 119603, doi: 10.1016/j.energy.2020.119603.
- [50] P. Wen, X. Li, N. Hou, and S. Mu, "Distributed recursive fault estimation with binary encoding schemes over sensor networks," *Syst. Sci. Control Eng.*, vol. 10, no. 1, pp. 417–427, Dec. 2022.
- [51] X. Lai, W. Yi, Y. Cui, C. Qin, X. Han, T. Sun, L. Zhou, and Y. Zheng, "Capacity estimation of lithium-ion cells by combining model-based and data-driven methods based on a sequential extended Kalman filter," *Energy*, vol. 216, Feb. 2021, Art. no. 119233, doi: 10.1016/j.energy.2020.119233.



YANJUN XIAO received the bachelor's degree in industrial automation and the master's degree in mechanical design manufacturing and automation from the Hebei University of Technology, in 2000 and 2009, respectively. From 2001 to 2007, he has worked with the Central Laboratory, School of Mechanical Engineering, Hebei University of Technology, where he has been a Professor, since 2017. He is currently teaching at the School of Mechanical Engineering, Hebei University of

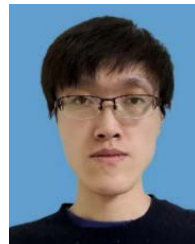
Technology, where he is also working with the Tianjin Key Laboratory of Power Transmission and Safety Technology for New Energy Vehicles. He is a professional with Jiangsu Career Leader Company Ltd. His main research interests include waste heat recovery and industrial control. He is in charge of Jiangsu Province Training Fund. He has won the 2017 and 2019 Hebei Science and Technology Invention Award and the Honorary Title of "Hebei Science and Technology Talent," in 2017.



SHUHAN DENG graduated from the Harbin University of Science and Technology, in 2020. He is currently pursuing the master's degree with the Hebei University of Technology. He mainly engaged in intelligent industrial connectivity and embedded development.



FURONG HAN received the graduate degree from the Hebei University of Technology, in 2020, where she is currently pursuing the master's degree. She is an Assistant Engineer with Jiangsu Career Leader Intelligent Control Automation Technology Company Ltd. Her research interests include intelligent control and health management.



XIAOLIANG WANG is currently pursuing the master's degree with the Hebei University of Technology. His major is electronic information. His research interests include embedded technology and intelligent control.



YUNFENG JIANG is currently pursuing the Ph.D. degree in engineering with the Hebei University of Technology. He is an Associate Researcher with the Hebei University of Technology. He is mainly engaged in scientific research in the field of mechanical manufacturing. He has produced a series of representative scientific research achievements in the direction of microfluidic chip technology and low-quality waste heat recovery technology. He has undertaken or participated in

the research of eight projects above the provincial and ministerial level, published more than 20 academic papers, and four authorized invention patents. He has won the Second Prize of Technological Invention of Hebei Province (the second adult).



KAI PENG received the Ph.D. degree in instrumentation engineering from Tianjin University. He is currently working as a Teacher at the Department of Measurement and Control, Hebei University of Technology, with the main research interests include geometric measurement technology, machine vision, and applications. He has published more than ten core papers, including three EI retrieved papers, more than ten authorized patents, and six copyrights. He has presided over

one provincial and ministerial-level project, five enterprise projects, and participated in or led three national projects and five provincial and ministerial-level projects. He has won the Hebei Science and Technology Award, the second prize, the main researcher, and the Hebei Challenge Cup for the excellent guidance teacher.

...